INTERNATIONAL JOURNAL OF
NUMERICAL ANALYSIS AND MODELING
Volume 2, Number 1, Pages 1–18

A POSTERIORI ERROR ESTIMATION FOR NON-CONFORMING QUADRILATERAL FINITE ELEMENTS

MARK AINSWORTH

(Communicated by Zhimin Zhang)

Abstract. We derive an a posteriori error estimator giving a computable upper bound on the error in the energy norm for finite element approximation using the non-conforming rotated $\mathbb{Q}_1$ finite element. It is shown that the estimator also gives a local lower bound up to a generic constant. The bounds do not require additional assumptions on the regularity of the true solution of the underlying elliptic problem and, the mesh is only required to be locally quasi-uniform and may consist of general, non-affine convex quadrilateral elements.

Key Words. A posteriori error estimation, non-conforming finite elements, rotated $\mathbb{Q}_1$ element, non-affine quadrilateral elements.

1. Introduction

Non-conforming finite element methods are of considerable interest in the numerical approximation of elliptic partial differential equations where issues of stability and locking [4] may render a conforming scheme practically useless. A large number of non-conforming finite element methods [7] were developed in the engineering community on a more or less *ad hoc* basis and found to produce excellent numerical results in practice. The mathematical support for such elements only came at a later stage, followed by the development of new non-conforming elements accompanied by proofs of stability and convergence [8, 14].

Whilst the topic of a posteriori error estimation for *conforming* finite element methods has now matured to a high level of sophistication [2, 3, 15], the situation regarding *non-conforming* finite element schemes is at a relatively primitive stage. An early important contribution to the theory of a posteriori error estimation for the non-conforming $\mathbb{P}_1$ triangular finite element of Crouzeix-Raviart [8] was made by Dari et. al. [10] who obtained two sided bounds on the error measured in the energy norm up to generic constants. These ideas were later extended to non-conforming mixed finite element approximation of Stokes flow [9] using the Crouzeix-Raviart finite element. Hierarchical basis type estimators were explored in [11], whilst [5] derived estimators based on gradient averaging techniques. More recently, a new a posteriori error estimator was derived [1] and shown to provide two-sided bounds on the error and, significantly, the upper bound does not involve *any* generic constants meaning that one has a guaranteed computable upper bound on the error measured in the energy norm.

Received by the editors October 6, 2004 and, in revised form, November 5, 2004.
2000 *Mathematics Subject Classification.* 65N50. Secondary 65N15, 65N50, 76S05.
Support for this work from the Leverhulme Trust through a Leverhulme Trust Fellowship is gratefully acknowledged.

The aim of the present work is to extend the ideas of [1] to the non-conforming *rotated* $\mathbb{Q}_1$ element of Rannacher and Turek [14] for meshes of quadrilaterals. The study of approximation properties on quadrilateral elements is rather delicate owing to the fact that the mapping from the standard reference element to the physical element is in general non-affine. This is exacerbated by the fact that, despite its name, the rotated $\mathbb{Q}_1$ element does not contain the full approximation space $\mathbb{Q}_1$, even in the case of affine elements. Together, these effects may even lead to non-convergence of the approximation error under certain unfavourable circumstances. Nevertheless, conditions on the mesh under which the element is able to produce an optimal rate of convergence are well-understood [12, 13] in the context of a priori error estimation where, roughly speaking, it is found that the elements should not be too distorted from parallelograms.

Here, we derive a computable a posteriori error estimator that produces an upper bound on the error in the energy norm that is valid even for non-affine elements. Moreover, it is shown that the estimator is efficient in the sense that it also gives a lower bound up to a generic constant independent of the mesh-size. The bounds are obtained without making any additional assumptions on the regularity of the true solution of the underlying elliptic problem, and the mesh is only required to be locally quasi-uniform, thereby allowing the use of an adaptive local refinement algorithm.

In view of the difficulties in the a priori convergence estimates, one might suspect the upper bound property of the a posteriori error estimator to degenerate on meshes containing elements that are too highly distorted. This proves not to be the case, and it is worth emphasising that our upper bound remains valid under the very mild assumption that the elements are convex. Of course, the effects of element distortion may well mean that, by analogy with the actual error, the estimator converges at a sub-optimal rate. This is to be expected from a reliable and efficient estimator, but it should be borne in mind that this is a defect of the underlying mesh and approximation scheme and not of the a posteriori error estimator. On the contrary, the availability of a computable upper bound means that one can actually use elements that are *more distorted* than one might have been comfortable with from the a priori viewpoint, secure in the knowledge that if the estimator is sufficiently small, then the overall approximation is acceptable thanks to the upper bound property of the estimator.

2. Model Problem and Its Non-conforming Discretisation

Consider the model problem of finding u such that

$$-\,\mathbf{div}(a\,\mathbf{grad}\,u) = f \quad \text{in } \Omega \tag{1}$$

subject to $u = 0$ on Γ_D and $\boldsymbol{n}\cdot a\,\mathbf{grad}\,u = g$ on Γ_N, where Ω is a planar polygonal domain and the disjoint sets Γ_D and Γ_N form a partitioning of the boundary of Ω. The data satisfy $f \in L_2(\Omega)$, $g \in L_2(\Gamma_N)$ and $a \in L_\infty(\Omega)$ is assumed non-negative. For simplicity, we shall assume that a is piecewise constant on the finite element mesh.

The variational form of the problem consists of seeking $u \in H^1_E(\Omega)$ such that

$$(a\,\mathbf{grad}\,u, \mathbf{grad}\,v) = (f, v) + \int_{\Gamma_N} gv\,\mathrm{d}s \quad \forall v \in H^1_E(\Omega) \tag{2}$$

where $H^1_E(\Omega) = \{v \in H^1(\Omega) : v = 0 \text{ on } \Gamma_D\}$. The notation $(\cdot,\cdot)_\omega$ is used to denote the L_2-inner product over a domain ω, with the subscript omitted where ω is the physical domain Ω. The corresponding norm is denoted by $\|\cdot\|_\omega$.

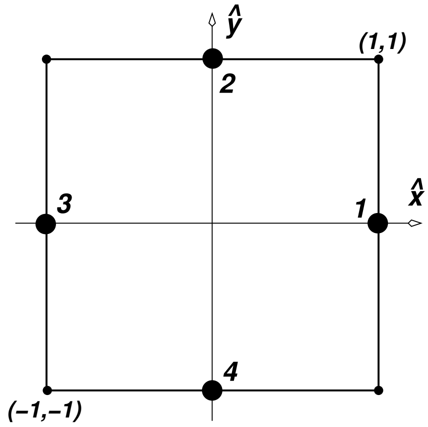

FIGURE 1. Geometry and degrees of freedom for rotated $\mathbb{Q}_1$ element

Let $\mathcal{P}$ denote a partitioning of the domain Ω into the disjoint union of convex quadrilateral elements such that the non-empty intersection of any two distinct elements is either a single common node or common edge. In addition, the non-empty intersection of an element with the exterior boundary is a portion of either Γ_D or Γ_N. The family of partitions is assumed to be locally quasi-uniform in the sense that the ratio of the diameters of any adjacent elements is bounded above and below uniformly over the whole family of partitions.

Each element $K \in \mathcal{P}$ is the image of the reference element $S = (-1,1)^2$ under an invertible bilinear mapping $\boldsymbol{F}_K : S \to K$. The elements are assumed to be regular in the sense that there exist positive constants c and C, independent of K, such that

$$\|D\boldsymbol{F}_K\|_{L_\infty(S)} \le Ch_K, \quad \|D\boldsymbol{F}_K^{-1}\|_{L_\infty(S)} \le Ch_K^{-1} \tag{3}$$

and

$$ch_K^2 \le \det(D\boldsymbol{F}_K) \le Ch_K^2 \text{ on } S \tag{4}$$

where h_K denotes the diameter of the element K and $D\boldsymbol{F}_K$ denotes the Jacobian matrix of the transformation $\boldsymbol{F}_K$. These conditions are investigated more fully in the Appendix.

The *rotated* $\mathbb{Q}_1$ *finite element* is defined by a triple (S, P, Σ) consisting of the reference element $S = (-1,1)^2$, the local polynomial space $P = \{1, \hat{x}, \hat{y}, \hat{x}^2 - \hat{y}^2\}$ and the set degrees of freedom Σ specified by function evaluation at the midpoints of the sides of S shown in Fig. 1. A Lagrange basis for the finite element is given by

$$\begin{aligned}
\hat{\phi}_1 &= \tfrac{1}{4} + \tfrac{1}{2}\hat{x} + \tfrac{1}{4}(\hat{x}^2 - \hat{y}^2)\\
\hat{\phi}_2 &= \tfrac{1}{4} + \tfrac{1}{2}\hat{y} - \tfrac{1}{4}(\hat{x}^2 - \hat{y}^2)\\
\hat{\phi}_3 &= \tfrac{1}{4} - \tfrac{1}{2}\hat{x} + \tfrac{1}{4}(\hat{x}^2 - \hat{y}^2)\\
\hat{\phi}_4 &= \tfrac{1}{4} - \tfrac{1}{2}\hat{y} - \tfrac{1}{4}(\hat{x}^2 - \hat{y}^2)
\end{aligned}$$

and satisfies the conditions $\hat{\phi}_k(\hat{\boldsymbol{m}}_\ell) = \delta_{k\ell}$, where $\{\hat{\boldsymbol{m}}_\ell\}$ consists of midpoints of edges.

The construction of the associated finite element space on a partitioning $\mathcal{P}$ is accomplished in the usual fashion. More specifically, let $\mathcal{N}$ index the set of element vertices, $\partial\mathcal{P}$ denote the set of element edges and $\mathcal{M} = \{\boldsymbol{m}_\gamma : \gamma \in \partial\mathcal{P}\}$ denote the set of points located at midpoints of edges. The *non-conforming rotated* $\mathbb{Q}_1$ *finite element space* is defined by

$$X_\mathcal{P} = \big\{v : \Omega \to \mathbb{R} : v_{|K} \circ \boldsymbol{F}_K \in P \quad \forall K \in \mathcal{P}, \quad v \text{ continuous at } \boldsymbol{m}_\gamma \in \mathcal{M}\backslash\partial\Omega\big\}$$

with the subspace $X_{\mathcal{P},E}$ defined by

$$X_{\mathcal{P},E} = \{v \in X_\mathcal{P} : v(\boldsymbol{m}_\gamma) = 0 \text{ for } \gamma \subset \Gamma_D\}\,.$$

The non-conforming finite element approximation of problem (2) consists of finding $u_\mathcal{P} \in X_{\mathcal{P},E}$ such that

$$(a\,\mathbf{grad}_\mathcal{P}\, u_\mathcal{P}, \mathbf{grad}_\mathcal{P}\, v) = (f, v) + \int_{\Gamma_N} gv\,\mathrm{d}s \quad \forall v \in X_{\mathcal{P},E} \tag{5}$$

where $\mathbf{grad}_\mathcal{P}$ denotes the operator defined by

$$(\mathbf{grad}_\mathcal{P}\, v)_{|K} = \mathbf{grad}(v_{|K}), \quad K \in \mathcal{P}.$$

The spaces $X_\mathcal{P}$ and $X_{\mathcal{P},E}$ are non-conforming in the sense that their elements may have jump discontinuities across inter-element boundaries and as a consequence, one does not have an internal approximation of the model problem.

The usual finite element interpolation operator associated with the finite element space $X_\mathcal{P}$ would be defined in terms of the values of the function to be approximated sampled at the midpoints $\mathcal{M}$. However, such an interpolant (i.e. involving sampling values pointwise) is not bounded on the space $H^1(\Omega)$. For this reason, it will be useful to consider an alternative interpolant defined in terms of average values of the traces of the function over edges. Standard results on traces show that the operator $\Pi_\mathcal{P} : H^1_E(\Omega) \to X_{\mathcal{P},E}$ is well-defined by the conditions

$$\int_\gamma \Pi_\mathcal{P} v\,\mathrm{d}s = \int_\gamma v\,\mathrm{d}s \quad \forall \gamma \in \partial\mathcal{P}. \tag{6}$$

More precisely, if the degrees of freedom Σ on the reference element are chosen to be average values over edges rather than function values at midpoints, then the corresponding Lagrange basis is given in terms of the nodal basis by

$$\begin{aligned}
\hat\psi_{\hat\gamma_1} &= \tfrac14 + \tfrac12\hat x + \tfrac38(\hat x^2 - \hat y^2)\\
\hat\psi_{\hat\gamma_2} &= \tfrac14 + \tfrac12\hat y - \tfrac38(\hat x^2 - \hat y^2)\\
\hat\psi_{\hat\gamma_3} &= \tfrac14 - \tfrac12\hat x + \tfrac38(\hat x^2 - \hat y^2)\\
\hat\psi_{\hat\gamma_4} &= \tfrac14 - \tfrac12\hat y - \tfrac38(\hat x^2 - \hat y^2)
\end{aligned} \tag{7}$$

and satisfies

$$\int_{\hat\gamma_\ell} \hat\psi_{\hat\gamma_k}\,\mathrm{d}s = 2\delta_{k\ell}$$

where $\{\hat\gamma_\ell\}$ are the edges of the reference element S. The corresponding global basis function ψ_γ associated with an edge $\gamma \in \partial\mathcal{P}$ is defined elementwise by

$$\psi_{\gamma\,|K} = \hat\psi_{\hat\gamma} \circ \boldsymbol{F}_K^{-1}, \quad \gamma = \boldsymbol{F}_K(\hat\gamma) \tag{8}$$

and satisfies the condition

$$\int_{\gamma'} \psi_\gamma\,\mathrm{d}s = h_\gamma \delta_{\gamma\gamma'}$$

where h_γ denotes the length of edge γ. The interpolation operator is then given explicitly by the expression

$$\Pi_{\mathcal{P}} v = \sum_{\gamma \subset \partial \mathcal{P}} \overline{v}_\gamma \psi_\gamma \tag{9}$$

where $\overline{v}_\gamma$ denotes the average value of v on an edge γ. Note that the restriction of $\Pi_{\mathcal{P}} v$ to a particular element K is locally defined (involving only averages of the function v on the edges of the particular element) and, in addition, $\Pi_{\mathcal{P}}$ locally preserves constants. For future reference, we note that this means that

$$\sum_{\gamma \subset \partial K} \psi_\gamma = (\Pi_{\mathcal{P}} 1)_{|K} = 1 \tag{10}$$

for each element $K \in \mathcal{P}$. Exploiting the above properties and applying standard scaling arguments leads to the conclusion that there exists a positive constant C depending only on the shape of the element such that the following local element-wise approximation property holds:

$$\|v - \Pi_{\mathcal{P}} v\|_K + h_K^{1/2} \|v - \Pi_{\mathcal{P}} v\|_{\partial K} \leq C h_K \|\mathbf{grad}\, v\|_K. \tag{11}$$

We shall make use of the following Poincaré inequality

$$\inf_{c \in \mathbb{R}} \|v - c\|_K \leq \mathcal{C}_p h_K \|\mathbf{grad}\, v\|_K \tag{12}$$

where $\mathcal{C}_p$ is a positive constant that depends only on the shape of the element and not its diameter h_K. In a similar vein, we shall make use of the following inequality relating the variation of the trace of a function over an edge γ of an element K to the gradient over the element

$$\inf_{c \in \mathbb{R}} \|v - c\|_\gamma \leq \mathcal{C}_t h_\gamma^{1/2} \|\mathbf{grad}\, v\|_K. \tag{13}$$

Bounds for $\mathcal{C}_p$ and $\mathcal{C}_t$ can be deduced from [6] or may be computed directly by solving an eigenvalue problem and exploiting the usual monotonicity properties of the eigenvalues with respect to the domain. It will be found that the constants will appear in the estimator as multiplicative factors in what will generally be higher order terms in the error estimator. This means that approximate upper bounds for $\mathcal{C}_p$ and $\mathcal{C}_t$ will be sufficient for practical purposes.

3. A Posteriori Error Analysis Framework

Our objective is to derive a computable estimator for the error $e = u - u_{\mathcal{P}}$ in the non-conforming approximation measured in the energy norm $|\!|\!| v |\!|\!|$ defined by

$$|\!|\!| v |\!|\!|^2 = (a\, \mathbf{grad}_{\mathcal{P}}\, v, \mathbf{grad}_{\mathcal{P}}\, v). \tag{14}$$

The following Helmholtz type decomposition (taken from Dari *et al.* [10]) will prove itself useful in this respect:

Lemma 1. *Let*

$$\mathcal{H} = \left\{ w \in H^1(\Omega) : \int_\Omega w \, \mathrm{d}\boldsymbol{x} = 0 \text{ and } \frac{\partial w}{\partial s} = 0 \text{ on } \Gamma_N \right\}.$$

The error e may be decomposed in the form

$$a\, \mathbf{grad}_{\mathcal{P}}\, e = a\, \mathbf{grad}\, \varepsilon + \mathbf{curl}\, \xi \tag{15}$$

where $\varepsilon \in H^1_E(\Omega)$ satisfies

$$(a\, \mathbf{grad}\, \varepsilon, \mathbf{grad}\, v) = (a\, \mathbf{grad}_{\mathcal{P}}\, e, \mathbf{grad}\, v) \quad \forall v \in H^1_E(\Omega) \tag{16}$$

and $\xi \in \mathcal{H}$ *satisfies*

$$(a^{-1}\,\mathbf{curl}\,\xi, \mathbf{curl}\,w) = (\mathbf{grad}_{\mathcal{P}}\,e, \mathbf{curl}\,w) \quad \forall w \in \mathcal{H} \tag{17}$$

where $\mathbf{curl}$ *denotes the operator* $\mathbf{curl}\,w = -\partial_y w\,\boldsymbol{e}_1 + \partial_x w\,\boldsymbol{e}_2$*. Moreover,*

$$|\!|\!|e|\!|\!|^2 = |\!|\!|\varepsilon|\!|\!|^2 + (a^{-1}\,\mathbf{curl}\,\xi, \mathbf{curl}\,\xi). \tag{18}$$

Lemma 1 shows that the error e in the non-conforming finite element approximation may be viewed as a sum of the projection ε of the total error onto the conforming space $H^1_E(\Omega)$ and referred to as the *conforming error*, plus a remainder ξ referred to as the *non-conforming error*. The orthogonality of the splitting with respect to the energy norm is an immediate consequence of the projection property. The practical import of the result is that it reduces the problem of obtaining a posteriori error estimators to the derivation of estimators for the conforming and non-conforming errors *independently*. An estimator for the total error is then given by summing the estimators for the independent contributions. This task will occupy us for the next two sections.

4. Estimation of Conforming Error

The conforming part $\varepsilon \in H^1_E(\Omega)$ of the error defined in equation (16). Equally well, by writing $e = u - u_{\mathcal{P}}$ and using the original equation (2), we have

$$(a\,\mathbf{grad}\,\varepsilon, \mathbf{grad}\,v) = (f, v) + \int_{\Gamma_N} gv\,\mathrm{d}s - (a\,\mathbf{grad}_{\mathcal{P}}\,u_{\mathcal{P}}, \mathbf{grad}\,v).$$

The interpolant defined in (6) satisfies $\Pi_{\mathcal{P}} : H^1_E(\Omega) \to X_{\mathcal{P},E}$ and, thanks to (5), we conclude that

$$0 = (f, \Pi_{\mathcal{P}} v) + \int_{\Gamma_N} g\Pi_{\mathcal{P}} v\,\mathrm{d}s - (a\,\mathbf{grad}_{\mathcal{P}}\,u_{\mathcal{P}}, \mathbf{grad}_{\mathcal{P}}\,\Pi_{\mathcal{P}} v)$$

and consequently,

$$(a\,\mathbf{grad}\,\varepsilon, \mathbf{grad}\,v) = \\ (f, v - \Pi_{\mathcal{P}} v) + \int_{\Gamma_N} g(v - \Pi_{\mathcal{P}} v)\,\mathrm{d}s - (a\,\mathbf{grad}_{\mathcal{P}}\,u_{\mathcal{P}}, \mathbf{grad}_{\mathcal{P}}(v - \Pi_{\mathcal{P}} v)).$$

Let $g_K \in L_2(\partial K)$ be defined by

$$g_K = \begin{cases} \dfrac{1}{2}\boldsymbol{n}_K \cdot (a_K\,\mathbf{grad}_{\mathcal{P}}\,u_{\mathcal{P}}|_K + a_{K'}\,\mathbf{grad}_{\mathcal{P}}\,u_{\mathcal{P}}|_{K'}) & \text{on } \gamma = \partial K \cap \partial K' \\ g & \text{on } \gamma \subset \Gamma_N \\ \boldsymbol{n}_K \cdot a_K\,\mathbf{grad}_{\mathcal{P}}\,u_{\mathcal{P}}|_K & \text{on } \gamma \subset \Gamma_D \end{cases}$$

then,

$$\sum_{K \in \mathcal{P}} \int_{\partial K} g_K(v - \Pi_{\mathcal{P}} v)\,\mathrm{d}s = \int_{\Gamma_N} g(v - \Pi_{\mathcal{P}} v)\,\mathrm{d}s, \quad v \in H^1_E(\Omega).$$

Hence,

$$(a\,\mathbf{grad}\,\varepsilon, \mathbf{grad}\,v) = \\ \sum_{K \in \mathcal{P}} \left\{ (f, v - \Pi_{\mathcal{P}} v)_K + \int_{\partial K} g_K(v - \Pi_{\mathcal{P}} v)\,\mathrm{d}s - (a\,\mathbf{grad}_{\mathcal{P}}\,u_{\mathcal{P}}, \mathbf{grad}_{\mathcal{P}}(v - \Pi_{\mathcal{P}} v))_K \right\}$$

and then integrating the final term by parts and simplifying, we find that

$$(a\,\mathbf{grad}\,\varepsilon, \mathbf{grad}\,v) = \sum_{K\in\mathcal{P}} \left\{ (r, v - \Pi_{\mathcal{P}} v)_K - \frac{1}{2}\int_{\partial K} J^{\nu}(v - \Pi_{\mathcal{P}} v)\,\mathrm{d}s \right\} \tag{19}$$

where r denotes the *interior* residual defined elementwise by

$$r_{|K} = f + \mathbf{div}_{\mathcal{P}}(a\,\mathbf{grad}_{\mathcal{P}}\,u_{\mathcal{P}}) \text{ on } K$$

and J^{ν} denotes the *jump* residual defined edgewise by

$$J^{\nu}_{|\gamma} = \begin{cases} \boldsymbol{n}_K \cdot \mathbf{grad}_{\mathcal{P}}\,u_{\mathcal{P}}|_K + \boldsymbol{n}_{K'} \cdot \mathbf{grad}_{\mathcal{P}}\,u_{\mathcal{P}}|_{K'} & \text{on } \gamma = \partial K \cap \partial K' \\ 2(g - \boldsymbol{n}_K \cdot \mathbf{grad}_{\mathcal{P}}\,u_{\mathcal{P}}|_K) & \text{on } \gamma = \partial K \cap \Gamma_N \\ 0 & \text{on } \gamma \subset \Gamma_D. \end{cases}$$

The equation (19) for the conforming error comprises of a volume term and a boundary term. The next step is to derive convenient representation formulae for each of these terms.

4.1. Representation of Volume Residual. Introduce vector-valued *interior* functions on the reference element S as follows

$$\widehat{\boldsymbol{\theta}}_1 = -\frac{3}{4}(1-\hat{x}^2)\boldsymbol{e}_1; \quad \widehat{\boldsymbol{\theta}}_2 = -\frac{3}{4}(1-\hat{y}^2)\boldsymbol{e}_2$$

and

$$\widehat{\boldsymbol{\theta}}_3 = -\frac{9}{16}\hat{y}(1-\hat{x}^2)\boldsymbol{e}_1 - \frac{9}{16}\hat{x}(1-\hat{y}^2)\boldsymbol{e}_2$$

where $\boldsymbol{e}_1$ and $\boldsymbol{e}_2$ are the unit cartesian basis vectors, along with *edge* functions associated with the boundary of S,

$$\widehat{\boldsymbol{\theta}}_{\hat{\gamma}_1} = \frac{1}{4}(\hat{x}+1)\boldsymbol{e}_1; \quad \widehat{\boldsymbol{\theta}}_{\hat{\gamma}_2} = \frac{1}{4}(\hat{y}+1)\boldsymbol{e}_2;$$

$$\widehat{\boldsymbol{\theta}}_{\hat{\gamma}_3} = \frac{1}{4}(\hat{x}-1)\boldsymbol{e}_1; \quad \widehat{\boldsymbol{\theta}}_{\hat{\gamma}_4} = \frac{1}{4}(\hat{y}-1)\boldsymbol{e}_2.$$

It is readily verified that normal components of the interior functions vanish on the boundary while the normal components of the edge functions satisfy

$$\hat{\boldsymbol{n}} \cdot \widehat{\boldsymbol{\theta}}_{\hat{\gamma}_k}\Big|_{\hat{\gamma}_\ell} = \frac{1}{2}\delta_{k\ell}, \quad 1 \le k \le 4, \quad 1 \le \ell \le 4$$

where $\hat{\boldsymbol{n}}$ denotes the unit outward normal on the boundary of S.

A corresponding set of functions is defined on a physical element K via the Piola transformation

$$\boldsymbol{\theta} = \frac{D\boldsymbol{F}_K}{\det(D\boldsymbol{F}_K)}\left(\widehat{\boldsymbol{\theta}} \circ \boldsymbol{F}_K^{-1}\right), \tag{20}$$

and thus, thanks to standard properties of the Piola transformation, it follows that these functions satisfy

$$\mathbf{div}\,\boldsymbol{\theta} = \frac{1}{\det(D\boldsymbol{F}_K)}\,\widehat{\mathbf{div}}\,\widehat{\boldsymbol{\theta}} \text{ in } K \tag{21}$$

where $\widehat{\mathbf{div}}$ denotes the divergence with respect to variables on the reference element, and

$$\boldsymbol{n}_K \cdot \boldsymbol{\theta}_{\gamma_k}|_{\gamma_\ell} = \frac{1}{|\gamma_\ell|}\delta_{k\ell}, \quad 1 \le k \le 4, \quad 1 \le \ell \le 4, \tag{22}$$

where $\boldsymbol{n}_K$ denotes the unit outward normal on the boundary of K, and $|\gamma_\ell|$ denotes the length of edge γ_ℓ. Of course, the normal components of the transformed interior functions remain zero.

The next result defines a weighted projection operator that turns out to be useful in measuring the data oscillation for non-affine elements. In the case of affine elements (where the Jacobian $D\boldsymbol{F}_K$ is constant) the operator is precisely orthogonal projection.

Lemma 2. *Let $r \in L_2(K)$ be given. Define $\pi_{\mathrm{K}}\, r \in L_2(K)$ by the rule*

$$\pi_{\mathrm{K}}\, r \circ \boldsymbol{F}_K^{-1} = \frac{1}{4\det(D\boldsymbol{F}_K)}\left[\alpha_0 + 6\alpha_1\hat{x} + 6\alpha_2\hat{y} + 9\alpha_3\hat{x}\hat{y}\right] \tag{23}$$

where

$$\alpha_0 = \int_K r\,\mathrm{d}\boldsymbol{x}; \quad \alpha_1 = \int_K r\hat{x}\,\mathrm{d}\boldsymbol{x}; \quad \alpha_2 = \int_K r\hat{y}\,\mathrm{d}\boldsymbol{x}; \quad \alpha_3 = \int_K r\hat{x}\hat{y}\,\mathrm{d}\boldsymbol{x} \tag{24}$$

with $\hat{\boldsymbol{x}} = \boldsymbol{F}_K^{-1}(\boldsymbol{x})$. Then,

$$\int_K (r - \pi_{\mathrm{K}}\, r)\hat{v}\,\mathrm{d}\boldsymbol{x} = 0, \quad \forall \hat{v} \in \{1, \hat{x}, \hat{y}, \hat{x}\hat{y}\}. \tag{25}$$

Proof. Elementary. □

The construction of the error estimator hinges on the following representation formula:

Lemma 3. *Let $r \in L_2(K)$ be given. Define $\boldsymbol{\sigma}_K \in \boldsymbol{L}_2(K)$ by*

$$\boldsymbol{\sigma}_K = \alpha_1\boldsymbol{\theta}_1 + \alpha_2\boldsymbol{\theta}_2 + \alpha_3\boldsymbol{\theta}_3 + \sum_{\gamma\subset\partial K}\alpha_\gamma\boldsymbol{\theta}_\gamma \tag{26}$$

where α_1, α_2 and α_3 are given in (24), and

$$\alpha_\gamma = \int_K r\psi_\gamma\,\mathrm{d}\boldsymbol{x}, \quad \gamma \subset \partial K \tag{27}$$

with ψ_γ defined as in (8). Then,

$$(\boldsymbol{\sigma}_K, \mathbf{grad}\, v)_K = \int_K r\,\Pi_{\mathcal{P}} v\,\mathrm{d}\boldsymbol{x} - \int_K (\pi_{\mathrm{K}}\, r)v\,\mathrm{d}\boldsymbol{x} \tag{28}$$

for all $v \in H^1(K)$, and

$$\|\boldsymbol{\sigma}_K\|_{a^{-1},K} \le Ch_K\|r\|_{a^{-1},K} \tag{29}$$

where $\|f\|_{a^{-1},K} = \|a^{-1/2}f\|_K$ for $K \in \mathcal{P}$, and C is a positive constant that is independent of the mesh-size.

Proof. Observing that thanks to (10), we have

$$\sum_{\gamma\subset\partial K}\alpha_\gamma = \int_K r\left(\sum_{\gamma\subset\partial K}\psi_\gamma\right)\mathrm{d}\boldsymbol{x} = \int_K r\,\mathrm{d}\boldsymbol{x} = \alpha_0,$$

and then making use of (21), we find that

$$\mathbf{div}\,\boldsymbol{\sigma} = \frac{1}{\det(D\boldsymbol{F}_K)}\left(\frac{3}{2}\alpha_1\hat{x} + \frac{3}{2}\alpha_2\hat{y} + \frac{9}{4}\alpha_3\hat{x}\hat{y} + \frac{1}{4}\sum_\gamma\alpha_\gamma\right) = \pi_{\mathrm{K}}\, r.$$

Moreover, thanks to (22), we have

$$\int_\gamma v\boldsymbol{n}\cdot\boldsymbol{\sigma}\,\mathrm{d}s = \alpha_\gamma\overline{v}_\gamma$$

where $\overline{v}_\gamma$ is the average value of v on γ and, applying (9), we have

$$\int_{\partial K} v\boldsymbol{n}\cdot\boldsymbol{\sigma}\,\mathrm{d}s = \sum_{\gamma\subset\partial K}\alpha_\gamma\overline{v}_\gamma = \int_K r\left(\sum_{\gamma\subset\partial K}\overline{v}_\gamma\psi_\gamma\right)\mathrm{d}\boldsymbol{x} = \int_K r\,\Pi_{\mathcal{P}}v\,\mathrm{d}\boldsymbol{x}.$$

The identity for $\boldsymbol{\sigma}_K$ now follows at once from the integration by parts formula

$$(\boldsymbol{\sigma}_K, \mathbf{grad}\, v)_K = \int_{\partial K} v\boldsymbol{n}\cdot\boldsymbol{\sigma}\,\mathrm{d}s - \int_K v\,\mathbf{div}\,\boldsymbol{\sigma}\,\mathrm{d}\boldsymbol{x}$$

on inserting the earlier results. The bound on the norm of $\boldsymbol{\sigma}_K$ is obtained by first observing that

$$\|\boldsymbol{\sigma}_K\|^2_{a^{-1},K} = \int_S \frac{1}{(a\circ\boldsymbol{F}_K)}\frac{1}{\det(D\boldsymbol{F}_K)}|D\boldsymbol{F}_K\widehat{\boldsymbol{\sigma}}_K|^2\,\mathrm{d}\hat{\boldsymbol{x}} \le \frac{C_K}{a_K}\|\widehat{\boldsymbol{\sigma}}\|^2_S$$

where

$$C_K = \frac{\|D\boldsymbol{F}_K\|^2_{L_\infty(S)}}{\min_S\det(D\boldsymbol{F}_K)}$$

is a constant that depends on the shape of the element K but not, thanks to assumptions (3)-(4), on the mesh-size. Applying the triangle inequality and bounding the coefficients α_k by $Ch_K\|r\|_K$, we obtain

$$a_K^{-1}\|\widehat{\boldsymbol{\sigma}}\|^2_S \le Ca_K^{-1}h_K^2\|r\|^2_K = Ch_K^2\|r\|^2_{a^{-1},K}$$

and the bound follows. □

4.2. Representation of Boundary Residual. Introduce scalar-valued functions on the reference element S as follows

(30) $$\hat{\vartheta}_1 = -\hat{y};\quad \hat{\vartheta}_2 = \hat{x};\quad \hat{\vartheta}_3 = \hat{x}\hat{y}$$

along with functions associated with the edges of S defined as follows

(31) $$\begin{aligned}\hat{\vartheta}_{\hat{\gamma}_1} &= \frac{3}{8}(1+\hat{x})(1-\hat{y}^2)\\ \hat{\vartheta}_{\hat{\gamma}_2} &= -\frac{3}{8}(1+\hat{y})(1-\hat{x}^2)\\ \hat{\vartheta}_{\hat{\gamma}_3} &= -\frac{3}{8}(1-\hat{x})(1-\hat{y}^2)\\ \hat{\vartheta}_{\hat{\gamma}_4} &= \frac{3}{8}(1-\hat{y})(1-\hat{x}^2).\end{aligned}$$

The function $\hat{\vartheta}_{\hat{\gamma}}$ vanishes everywhere on the boundary of S apart from the edge $\hat{\gamma}$. Let ϑ denote the usual pull-back of $\hat{\vartheta}$ defined on element K by $\vartheta = \hat{\vartheta}\circ\boldsymbol{F}_K^{-1}$.

By analogy with the interior residual, we shall need a projection operator on the boundary to measure the data oscillation. However, the simpler structure of the approximation on the boundary means that we have a standard orthogonal projection this time.

Lemma 4. *Let $\gamma\subset\partial K$ and $G\in L_2(\gamma)$ be given. Then,*

(32) $$\pi_\gamma\, G = \frac{1}{h_\gamma}\int_\gamma G\,\mathrm{d}s + 3\frac{\hat{x}_\gamma}{h_\gamma}\int_\gamma G\hat{x}_\gamma\,\mathrm{d}s$$

satisfies

(33) $$\int_\gamma (G-\pi_\gamma\, G)\hat{v}\,\mathrm{d}s = 0,\quad \forall\hat{v}\in\{1,\hat{x}_\gamma\}$$

where $\hat{x}_\gamma\in(-1,1)$ is the reference coordinate on the edge γ.

Proof. Elementary. □

The following representation formula will be used to handle the boundary residual:

Lemma 5. *Define*

$$\chi_K = \beta_1\vartheta_1 + \beta_2\vartheta_2 + \beta_3\vartheta_3 + \sum_{\gamma\subset\partial K}\beta_\gamma\vartheta_\gamma \tag{34}$$

where

$$\beta_1 = \frac{1}{4}(\rho_1-\rho_3); \quad \beta_2 = \frac{1}{4}(\rho_2-\rho_4); \quad \beta_3 = -\frac{1}{8}(\rho_1-\rho_2+\rho_3-\rho_4) \tag{35}$$

and

$$\rho_k = \int_{\gamma_k} J^\nu \,\mathrm{d}s - \int_{\partial K} J^\nu \psi_{\gamma_k}\,\mathrm{d}s \tag{36}$$

with

$$\beta_\gamma = \int_\gamma J^\nu\,\hat{x}_\gamma\,\mathrm{d}s, \quad \gamma\subset\partial K \tag{37}$$

where $\hat{x}_\gamma \in (-1,1)$ *is the reference coordinate on edge* γ*. Then,*

$$(\mathbf{curl}\,\chi_K, \mathbf{grad}\,v)_K = \sum_{\gamma\subset\partial K}\int_\gamma (\pi_\gamma\, J^\nu)\,v\,\mathrm{d}s - \int_{\partial K} J^\nu\,\Pi_{\mathcal{P}} v\,\mathrm{d}s \tag{38}$$

for all $v \in H^1(K)$*, and there exists a positive constant* C *such that*

$$\|\mathbf{curl}\,\chi_K\|_{a^{-1},K} \le C\sum_{\gamma\subset\partial K} h_\gamma^{1/2}\|J^\nu\|_{a^{-1},\gamma} \tag{39}$$

where $\|g\|_{a^{-1},\gamma} = \|a_\gamma^{-1/2} g\|_\gamma$ *and* $a_\gamma = \max\{a_K : \gamma\in\partial K\}$*.*

Proof. Observe that

$$\mathbf{curl}\,\chi_K = \frac{D\boldsymbol{F}_K}{\det(D\boldsymbol{F}_K)}\,\widehat{\mathbf{curl}}\,\hat{\chi}_K$$

and

$$\boldsymbol{n}\cdot\mathbf{curl}\,\chi_K = \frac{2}{h_\gamma}\hat{\boldsymbol{n}}_\gamma\cdot\widehat{\mathbf{curl}}\,\hat{\chi}_K = -\frac{2}{h_\gamma}\frac{\partial\hat{\chi}_K}{\partial\hat{s}}$$

where $\hat{s}$ denotes arclength on the reference element. Consequently, integrating by parts gives

$$(\mathbf{curl}\,\chi_K, \mathbf{grad}\,v)_K = \int_{\partial K} v\boldsymbol{n}\cdot\mathbf{curl}\,\chi_K\,\mathrm{d}s = \sum_{\gamma\subset\partial K} -\frac{2}{h_\gamma}\int_\gamma v\frac{\partial\hat{\chi}_K}{\partial\hat{s}}\,\mathrm{d}s.$$

A direct computation reveals that on each edge $\gamma\subset\partial K$,

$$\left.\frac{\partial\hat{\chi}_K}{\partial\hat{s}}\right|_\gamma = -\frac{1}{2}\rho_\gamma - \frac{3}{2}\hat{x}_\gamma\beta_\gamma$$

where we have made use of the fact that

$$\sum_{\gamma\subset\partial K}\rho_\gamma = \sum_{\gamma\subset\partial K}\int_\gamma J^\nu\,\mathrm{d}s - \int_{\partial K} J^\nu\left(\sum_{\gamma\subset\partial K}\psi_\gamma\right) = 0$$

since the term in parentheses is unity, thanks to (10). Simplifying, we have

$$\left.\frac{\partial\hat{\chi}_K}{\partial\hat{s}}\right|_\gamma = \frac{1}{2}\int_{\partial K} J^\nu\psi_\gamma\,\mathrm{d}s - \frac{1}{2}\int_\gamma J^\nu\,\mathrm{d}s - \frac{3}{2}\hat{x}_\gamma\int_\gamma J^\nu\hat{x}_\gamma\,\mathrm{d}s.$$

Therefore, in view of (32), we find

$$-\frac{2}{h_\gamma}\frac{\partial\hat{\chi}_K}{\partial\hat{s}}\bigg|_\gamma = -\frac{1}{h_\gamma}\int_{\partial K} J^\nu \psi_\gamma \,\mathrm{d}s + (\pi_\gamma\, J^\nu)_{|\gamma}\,.$$

Furthermore,

$$\sum_{\gamma\subset\partial K}\frac{1}{h_\gamma}\int_{\partial K} J^\nu\psi_\gamma\,\mathrm{d}s\int_\gamma v\,\mathrm{d}s = \int_{\partial K} J^\nu\left(\sum_\gamma \overline{v}_\gamma\psi_\gamma\right)\mathrm{d}s = \int_{\partial K} J^\nu \Pi_{\mathcal{P}} v\,\mathrm{d}s$$

and the identity follows at once on collecting the foregoing results. The bound for the norm of $\mathbf{curl}\,\chi_K$ is obtained using essentially the same argument as the one used to derive (29) after bounding the coefficients β_k by $\sum_{\gamma\subset\partial K} h_\gamma^{1/2}\|J^\nu\|_\gamma$. □

4.3. A Posteriori Error Bounds. We now come to the main result of this section giving two-sided bounds on the conforming part of the error.

Theorem 1. *Let $r\in L_2(K)$ and $J^\nu\in L_2(\partial K)$ denote the interior residual and inter-element flux jump respectively, and define $\boldsymbol{\sigma}_K$ and χ_K as in Lemmas 3 and 4. Then,*

$$\interleave\varepsilon\interleave^2 \le \sum_{K\in\mathcal{P}}\left(\|\boldsymbol{\sigma}_K + \frac{1}{2}\mathbf{curl}\,\chi_K\|_{a^{-1},K} + \Delta_K\right)^2 \tag{40}$$

where

$$\Delta_K = \mathcal{C}_p h_K\|r-\pi_{\mathrm{K}}\, r\|_{a^{-1},K} + \frac{1}{2}\mathcal{C}_t\sum_{\gamma\subset\partial K} h_\gamma^{1/2}\|J^\nu - \pi_\gamma\, J^\nu\|_{a^{-1},\gamma}. \tag{41}$$

Moreover, there exists a positive constant c, independent of any mesh-size, such that for each element $K\in\mathcal{P}$, there holds

$$c\|\boldsymbol{\sigma}_K + \frac{1}{2}\mathbf{curl}\,\chi_K\|_{a^{-1},K} \le \interleave\varepsilon\interleave_{\widetilde{K}} + \Delta_K \tag{42}$$

where $\widetilde{K}$ is the patch comprising of the element K and its neighbours.

Proof. For all $v\in H^1_E(\Omega)$, the conforming part of the error $\varepsilon\in H^1_E(\Omega)$ satisfies

$$(a\,\mathbf{grad}\,\varepsilon,\mathbf{grad}\,v) = \sum_{K\in\mathcal{P}}\left\{(r, v-\Pi_{\mathcal{P}}v)_K - \frac{1}{2}\int_{\partial K} J^\nu(v-\Pi_{\mathcal{P}}v)\,\mathrm{d}s\right\}.$$

Applying Lemmas 3 and 4, we obtain

$$(r, v-\Pi_{\mathcal{P}}v)_K - \frac{1}{2}\int_{\partial K} J^\nu(v-\Pi_{\mathcal{P}}v)\,\mathrm{d}s = -(\boldsymbol{\sigma}_K + \frac{1}{2}\mathbf{curl}\,\chi_K, \mathbf{grad}\,v)_K + (r-\pi_{\mathrm{K}}\, r, v)_K - \frac{1}{2}\sum_{\gamma\subset\partial K}\int_\gamma (J^\nu - \pi_\gamma\, J^\nu)v\,\mathrm{d}s.$$

The terms appearing above are estimated in turn as follows. The first term is bounded directly using the Cauchy-Schwarz inequality

$$-(\boldsymbol{\sigma}_K + \frac{1}{2}\mathbf{curl}\,\chi_K, \mathbf{grad}\,v)_K \le \|\boldsymbol{\sigma}_K + \frac{1}{2}\mathbf{curl}\,\chi_K\|_{a^{-1},K}\,\interleave v\interleave_K\,.$$

The second term is bounded by first exploiting property (25) to write

$$(r-\pi_{\mathrm{K}}\, r, v)_K = (r-\pi_{\mathrm{K}}\, r, v-c)_K$$

for arbitrary $c \in \mathbb{R}$. Then, applying the Cauchy-Schwarz inequality, taking the infimum over c and using the Poincaré inequality (12), we obtain

$$\begin{aligned}(r - \pi_{\mathrm{K}}\, r, v)_K &\leq \mathcal{C}_p h_K \|r - \pi_{\mathrm{K}}\, r\|_K \|\mathbf{grad}\, v\|_K \\ &= \mathcal{C}_p h_K \|r - \pi_{\mathrm{K}}\, r\|_{a^{-1},K} \, |\!|\!| v |\!|\!|_K \,.\end{aligned}$$

The third term is treated similarly by first writing

$$\int_\gamma (J^\nu - \pi_\gamma\, J^\nu) v \,\mathrm{d}s = \int_\gamma (J^\nu - \pi_\gamma\, J^\nu)(v - c) \,\mathrm{d}s$$

for $c \in \mathbb{R}$, and arguing as above using inequality (13), we arrive at

$$\begin{aligned}-\int_\gamma (J^\nu - \pi_\gamma\, J^\nu) v \,\mathrm{d}s &\leq \mathcal{C}_t h_\gamma^{1/2} \|J^\nu - \pi_\gamma\, J^\nu\|_\gamma \|\mathbf{grad}\, v\|_K \\ &= \mathcal{C}_t h_\gamma^{1/2} \|J^\nu - \pi_\gamma\, J^\nu\|_{a^{-1},\gamma} \, |\!|\!| v |\!|\!|_K \,.\end{aligned}$$

The upper bound for $|\!|\!| \varepsilon |\!|\!|$ follows at once on choosing $v = \varepsilon \in H^1_E(\Omega)$, summing the above estimates over all elements and applying the Cauchy-Schwarz inequality.

The lower bound is obtained by applying the triangle inequality and estimates (29) and (39) to give

$$c\|\boldsymbol{\sigma}_K + \frac{1}{2}\,\mathbf{curl}\, \chi_K\|_{a^{-1},K} \leq h_K \|r\|_{a^{-1},K} + \sum_{\gamma \subset \partial K} h_\gamma^{1/2} \|J^\nu\|_{a^{-1},\gamma}.$$

Bounds for the terms appearing above are obtained using the residual equation (19) and a standard 'bubble' function argument (see, for example, [2, Section 2.3]) leading to

$$c h_K \|r\|_{a^{-1},K} \leq |\!|\!| \varepsilon |\!|\!|_K + h_K \|r - \pi_{\mathrm{K}}\, r\|_{a^{-1},K}$$

and

$$\begin{aligned}&c h_\gamma^{1/2} \|J^\nu\|_{a^{-1},\gamma} \leq \\ &\qquad |\!|\!| \varepsilon |\!|\!|_{\tilde{\gamma}} + h_\gamma^{1/2} \|J^\nu - \pi_\gamma\, J^\nu\|_{a^{-1},\gamma} + \sum_{K \subset \tilde{\gamma}} h_K \|r - \pi_{\mathrm{K}}\, r\|_{a^{-1},K}\end{aligned}$$

where c is a positive constant independent of any mesh-size. Inserting these bounds into the above estimate leads to the local lower bound on the error claimed. □

5. Estimation of Non-Conforming Error

The next result will be helpful in deriving bounds for the non-conforming contribution ξ to the total error:

Lemma 6. *Let $\xi \in \mathcal{H}$ be defined as in* (17). *Then,*

$$(a^{-1}\,\mathbf{curl}\,\xi, \mathbf{curl}\,\xi) = \min_{u^* \in H^1_E(\Omega)} |\!|\!| u^* - u_{\mathcal{P}} |\!|\!|^2 \,. \tag{43}$$

The proof of the result can be found in [1]. Evidently, inserting *any* function $u^* \in H^1_E(\Omega)$ into the right hand side of (43) gives an upper bound on the non-conforming part of the error. However, if one is to obtain an efficient upper bound, then some care has to be exercised in the choice of u^*. Furthermore, if the bound is to be readily calculable, then it is necessary for the function u^* to have a reasonably simple form.

Bearing these considerations in mind, u^* is taken to be a piecewise (pull-back) biquadratic function on the partition $\mathcal{P}$. The function is fully specified once the values at the element vertices, edge midpoints and element centroids are defined.

The values at a vertex located on the Dirichlet boundary Γ_D are predetermined by the requirement $u^* \in H^1_E(\Omega)$. At one of the remaining vertices, at say $\boldsymbol{x}_n$, $n \in \mathcal{N}$, the finite element approximation $u_{\mathcal{P}}$ will in general be discontinuous. Let $\Omega_n \subset \mathcal{P}$ denote the set of elements that have $\boldsymbol{x}_n$ as one of their vertices. The value of u^* at vertex is defined to be the average of the values of the finite element approximation $u_{\mathcal{P}}$ at the vertex,

$$u^*(\boldsymbol{x}_n) = \begin{cases} 0, & \text{if } \boldsymbol{x}_n \in \Gamma_D \\ \dfrac{1}{|\mathcal{P}_n|} \displaystyle\sum_{K \in \mathcal{P}_n} u_{\mathcal{P}}(\boldsymbol{x}_n)_{|K}, & \text{otherwise.} \end{cases} \tag{44}$$

where $|\mathcal{P}_n|$ denotes the number of elements in the set $\mathcal{P}_n$. The finite element approximation is continuous at edge midpoints and there is no ambiguity in defining the value of u^* at the midpoints according to the rule

$$u^*(\boldsymbol{m}_\gamma) = \begin{cases} 0, & \text{if } \boldsymbol{m}_\gamma \in \Gamma_D \\ u_{\mathcal{P}}(\boldsymbol{m}_\gamma), & \text{otherwise.} \end{cases} \tag{45}$$

Finally, the finite element approximation is single-valued within each element, and we may therefore define

$$u^*(\overline{\boldsymbol{x}}_K) = u_{\mathcal{P}}(\overline{\boldsymbol{x}}_K), \quad \forall K \in \mathcal{P} \tag{46}$$

where $\overline{\boldsymbol{x}}_K$ denotes the centroid of element K.

With these definitions, it follows that $u^* \in H^1_E(\Omega)$ and may be used to obtain an upper bound for the non-conforming contribution to the error.

We now turn to the efficiency of the estimator.

Theorem 2. *Let $u^* \in H^1_E(\Omega)$ be constructed as described above. Then,*

$$\|\mathbf{curl}\,\xi\|_{a^{-1},\Omega} \leq \| u_{\mathcal{P}} - u^* \| \tag{47}$$

and, moreover, there exists a positive constant c, independent of any mesh-size, such that

$$\| u_{\mathcal{P}} - u^* \|_K \leq C\|\mathbf{curl}\,\xi\|_{a^{-1},\widetilde{K}}. \tag{48}$$

Proof. The upper bound is an immediate consequence of the preceding arguments. Some preparation will be needed for the lower bound.

The jump J^τ in the tangential derivative on an edge γ is defined by

$$J^\tau_{|\gamma} = \begin{cases} \boldsymbol{t}_K \cdot \mathbf{curl}\, u_{\mathcal{P}}|_K + \boldsymbol{t}_{K'} \cdot \mathbf{curl}\, u_{\mathcal{P}}|_{K'} & \text{on } \gamma = \partial K \cap \partial K' \\ \boldsymbol{t}_K \cdot \mathbf{grad}\, u_{\mathcal{P}}|_K & \text{on } \gamma = \partial K \cap \Gamma_D \\ 0 & \text{on } \gamma \subset \Gamma_N \end{cases}$$

where $\boldsymbol{t}_K$ denotes the unit tangent vector on ∂K, taken in an anti-clockwise sense. Let $\gamma \in \partial K - \Gamma_N$ be any edge that is not located on the Neumann boundary and let β_γ denote the pull-back quadratic function associated with the midpoint of γ. Since the mapping $\hat{\gamma} \to \gamma = \boldsymbol{F}_K(\hat{\gamma})$ is affine, it follows that $u_{\mathcal{P}}|_\gamma$ is quadratic and hence, J^τ_γ is quadratic. Let $\beta_\gamma J^\tau_\gamma$ denote the usual extension of J^τ to the element(s) neighbouring edge γ. Then, a scaling argument (see, e.g. [2, Section 2.3]) shows that

$$c h_\gamma^{-1/2} \|\mathbf{curl}(\beta_\gamma J^\tau_\gamma)\|_{\tilde{\gamma}} \leq \|J^\tau_\gamma\|_\gamma \leq C\|\beta_\gamma^{1/2} J^\tau_\gamma\|_\gamma \tag{49}$$

where c and C are positive constants independent of any mesh-size. Now, let $w \in \mathcal{H}$ be the difference between $\beta_\gamma J_\gamma^\tau$ and its constant average value over Ω. This choice of w in (17) gives

$$(a^{-1}\,\mathbf{curl}\,\xi, \mathbf{curl}(\beta_\gamma J_\gamma^\tau)) = (\mathbf{grad}_\mathcal{P}\, e, \mathbf{curl}(\beta_\gamma J_\gamma^\tau))$$

and then writing the right hand as a sum of contributions from individual elements $K \subset \tilde{\gamma}$, integrating by parts and noting that the true solution $u \in H_E^1(\Omega)$, we obtain

$$(a^{-1}\,\mathbf{curl}\,\xi, \mathbf{curl}(\beta_\gamma J_\gamma^\tau)) = \int_\gamma \beta_\gamma (J_\gamma^\tau)^2\,\mathrm{d}s.$$

Applying the Cauchy-Schwarz inequality and making use of (49) we arrive at

$$c\|J^\tau\|_\gamma^2 \leq \|a^{-1}\,\mathbf{curl}\,\xi\|_{\tilde{\gamma}}\|\mathbf{curl}(\beta_\gamma J^\tau)\|_{\tilde{\gamma}} \leq C h_\gamma^{-1/2}\|a^{-1}\,\mathbf{curl}\,\xi\|_{\tilde{\gamma}}\|J^\tau\|_\gamma$$

and hence,

$$h_\gamma^{1/2}\|J_\gamma^\tau\|_\gamma \leq C\|a^{-1}\,\mathbf{curl}\,\xi\|_{\tilde{\gamma}}. \tag{50}$$

Suppose that distinct elements K and K' share the common edge γ. Then, since $u_\mathcal{P}$ is continuous at the midpoint $\boldsymbol{m}_\gamma$,

$$|u_\mathcal{P}(\boldsymbol{x}_n)_{|K'} - u_\mathcal{P}(\boldsymbol{x}_n)_{|K}| = \left|\int_{\boldsymbol{m}_\gamma}^{\boldsymbol{x}_n} J_\gamma^\tau\,\mathrm{d}s\right|.$$

Hence, by a Cauchy-Schwarz inequality,

$$|u_\mathcal{P}(\boldsymbol{x}_n)_{|K'} - u_\mathcal{P}(\boldsymbol{x}_n)_{|K}| \leq h_\gamma^{1/2}\|J_\gamma^\tau\|_\gamma$$

and applying (50), we have

$$|u_\mathcal{P}(\boldsymbol{x}_n)_{|K'} - u_\mathcal{P}(\boldsymbol{x}_n)_{|K}| \leq \|a^{-1}\,\mathbf{curl}\,\xi\|_{\tilde{\gamma}}, \quad \boldsymbol{x}_n \in \gamma = \partial K \cap \partial K'. \tag{51}$$

Suppose that element K has an edge γ on the Dirichlet portion of the boundary. Then, since $u_\mathcal{P}(\boldsymbol{m}_\gamma)$ vanishes,

$$|u_\mathcal{P}(\boldsymbol{x}_n)_{|K}| = \left|\int_{\boldsymbol{m}_\gamma}^{\boldsymbol{x}_n} J_\gamma^\tau\,\mathrm{d}s\right|$$

and arguing as before, we obtain

$$|u_\mathcal{P}(\boldsymbol{x}_n)_{|K}| \leq \|a^{-1}\,\mathbf{curl}\,\xi\|_{\tilde{\gamma}}, \quad \boldsymbol{x}_n \in \gamma = \partial K \cap \Gamma_N \tag{52}$$

We now turn to the efficiency of the estimator on an element $K \in \mathcal{P}$. Both $u_{\mathcal{P}|K}$ and $u^*_{|K}$ are pull-back biquadratic functions on K whose values agree at the element centroid and edge midpoints. That is, the difference $u_\mathcal{P} - u^*$ on an element $K \in \mathcal{P}$ vanishes at the centroid and edge midpoints, and may therefore be written in the form

$$(u_\mathcal{P} - u^*)_{|K} = \sum_{n\in\mathcal{N}(K)} c_n^{(K)}\theta_n^*$$

where θ_n^* is the pull-back biquadratic approximation associated with vertex n, and

$$c_n^{(K)} = \frac{1}{|\mathcal{P}_n|}\sum_{K'\in\mathcal{P}_n}\left(u_\mathcal{P}(\boldsymbol{x}_n)_{|K'} - u_\mathcal{P}(\boldsymbol{x}_n)_{|K}\right)$$

for $\boldsymbol{x}_n \notin \Gamma_D$ and $c_n^{(K)} = -u_\mathcal{P}(\boldsymbol{x}_n)_{|K}$ if $\boldsymbol{x}_n \in \Gamma_D$. By writing the difference $u_\mathcal{P}(\boldsymbol{x}_n)_{|K'} - u_\mathcal{P}(\boldsymbol{x}_n)_{|K}$ as a telescoping sum of differences of values between neighbouring elements, and then applying estimates (51) and (52) as needed, we arrive at the estimate

$$|c_n^{(K)}| \leq \|a^{-1}\,\mathbf{curl}\,\xi\|_{\Omega_n},$$

which holds regardless of the location of $\boldsymbol{x}_n$.

Standard scaling arguments reveal that $\|\theta_n^*\|$ is independent of the element size and therefore, with the aid of the triangle inequality,

$$\|u_{\mathcal{P}} - u^*\|_K \leq C \sum_{n \in \mathcal{N}(K)} |c_n^{(K)}| \, \|\theta_n^*\|_K \leq C \|\mathbf{curl}\, \xi\|_{a^{-1},\widetilde{K}}$$

where the constant is independent of the coefficient a and any mesh-size. □

6. Summary and Practical Application of the Theory

Applying Lemma 1 and Theorems 1 and 2, we obtain the following upper bound for the total error

$$\|e\|^2 \leq \sum_{K \in \mathcal{P}} (\|\boldsymbol{\sigma}_K + \frac{1}{2}\mathbf{curl}\, \chi_K\|_{a^{-1},K}^2 + \Delta_K)^2 + \|u_{\mathcal{P}} - u^*\|^2 \tag{53}$$

along with corresponding local lower bounds.

Given an element $K \in \mathcal{P}$, we evaluate the functions $\widehat{\boldsymbol{\sigma}}_K$ and $\hat{\chi}_K$ defined in Lemmas 3 and 5 in terms of the local residual $r_{|K}$ and the jump J_γ^ν in the normal flux over the element boundary. The estimator for the conforming part of the error is then obtained by evaluating

$$\begin{aligned} &\|\boldsymbol{\sigma}_K + \frac{1}{2}\mathbf{curl}\, \chi_K\|_{a^{-1},K}^2 = \\ &\frac{1}{a_K}\int_S (\widehat{\boldsymbol{\sigma}}_K + \frac{1}{2}\widehat{\mathbf{curl}}\, \hat{\chi}_K)^\top \boldsymbol{G}_K(\hat{\boldsymbol{x}})(\widehat{\boldsymbol{\sigma}}_K + \frac{1}{2}\widehat{\mathbf{curl}}\, \hat{\chi}_K)\, \mathrm{d}\hat{\boldsymbol{x}} \end{aligned} \tag{54}$$

where $\boldsymbol{G}_K$ is the matrix defined by

$$\boldsymbol{G}_K(\hat{\boldsymbol{x}}) = \frac{1}{\det(D\boldsymbol{F}_K)} D\boldsymbol{F}_K(\hat{\boldsymbol{x}})^\top D\boldsymbol{F}_K(\hat{\boldsymbol{x}})$$

and studied in the Appendix. For an affine element, this integral may be evaluated exactly using numerical quadrature, but this will not always be the case and there is a danger that the upper bound property will be lost due to inexact quadrature. An alternative approach is to use the bound

$$\boldsymbol{G}_K(\hat{\boldsymbol{x}}) \leq \frac{1}{1 - \widehat{\delta}_K}\boldsymbol{G}_K(\mathbf{0}).$$

This bound is to be understood in terms of the values of the corresponding quadratic forms induced by the matrices, and is proven in the Appendix where $\widehat{\delta}_K$ is also defined and shown to depend on the amount by which the element is distorted from an affine element but not on any mesh-size. In particular, $\widehat{\delta}_K$ vanishes in the case of an affine element. The resulting contribution to the error estimator becomes

$$\frac{1}{a_K}(1 - \widehat{\delta}_K)^{-1}\int_S (\widehat{\boldsymbol{\sigma}}_K + \frac{1}{2}\widehat{\mathbf{curl}}\, \hat{\chi}_K)^\top \boldsymbol{G}_K(\mathbf{0})(\widehat{\boldsymbol{\sigma}}_K + \frac{1}{2}\widehat{\mathbf{curl}}\, \hat{\chi}_K)\, \mathrm{d}\hat{\boldsymbol{x}} \tag{55}$$

and provides an upper bound that can be evaluated exactly using numerical quadrature. The efficiency of the estimator is unaffected by this change thanks to the assumptions (3)-(4) on the elements.

The upper bound also involves the data oscillation term

$$\Delta_K = \mathcal{C}_p h_K \|r - \pi_K\, r\|_{a^{-1},K} + \frac{1}{2}\mathcal{C}_t \sum_{\gamma \subset \partial K} h_\gamma^{1/2} \|J^\nu - \pi_\gamma\, J^\nu\|_{a^{-1},\gamma}.$$

The terms appearing in the norms mean that Δ_K will often be of higher order, or even negligible, compared with the previous contribution to the estimator. The norms appearing in this quantity could be computed directly, but bounds are needed for the constants $\mathcal{C}_p$ and $\mathcal{C}_t$. It is unnecessary to obtain the sharpest possible bounds for these constants since the norms are relatively small and over-estimation of the constants is unlikely to detrimentally affect the estimator in practice. The usual approach is to to simply neglect this term completely when evaluating the estimator.

The estimator for the non-conforming contribution to the error involves computation of values of the post-processed approximation u^* at element vertices. Once again, the possibility arises of inexact quadrature compromising the upper bounds. Now,

$$|||u_{\mathcal{P}} - u^*|||_K^2 = a_K \int_K \mathbf{grad}(u_{\mathcal{P}} - u^*)^\top \, \mathbf{grad}(u_{\mathcal{P}} - u^*) \, \mathrm{d}\boldsymbol{x}$$

and denoting the push-forward of $u_{\mathcal{P}} - u^*$ on element K by $\hat{u}$, we obtain

$$|||u_{\mathcal{P}} - u^*|||_K^2 = a_K \int_S (\widehat{\mathbf{grad}}\, \hat{u})^\top \boldsymbol{G}_K(\hat{\boldsymbol{x}})^{-1} (\widehat{\mathbf{grad}}\, \hat{u}) \, \mathrm{d}\hat{\boldsymbol{x}}$$

where the matrix $\boldsymbol{G}_K(\hat{\boldsymbol{x}})$ is defined above. Applying the lower bound

$$\boldsymbol{G}_K(\hat{\boldsymbol{x}}) \geq (1 - \widehat{\delta}_K)\boldsymbol{G}_K(\mathbf{0})$$

from the Appendix, we obtain

$$|||u_{\mathcal{P}} - u^*|||_K^2 \leq a_K(1 - \widehat{\delta}_K)^{-1} \int_S (\widehat{\mathbf{grad}}\, \hat{u})^\top \boldsymbol{G}_K(\mathbf{0})^{-1} (\widehat{\mathbf{grad}}\, \hat{u}) \, \mathrm{d}\hat{\boldsymbol{x}}.$$

As before, the integral may be evaluated exactly using numerical quadrature and the integrity of the upper bound property is not compromised.

7. Appendix

Let $K \in \mathcal{P}$ be any element satisfying conditions (3)-(4). Let $\boldsymbol{F}_K$ denote the bilinear mapping from the reference element S onto the element. The matrix $\boldsymbol{G}_K$ is defined by

$$\boldsymbol{G}_K(\hat{\boldsymbol{x}}) = \frac{1}{\det(D\boldsymbol{F}_K(\hat{\boldsymbol{x}}))} D\boldsymbol{F}_K(\hat{\boldsymbol{x}})^\top D\boldsymbol{F}_K(\hat{\boldsymbol{x}}), \quad \hat{\boldsymbol{x}} \in S \tag{56}$$

where $D\boldsymbol{F}_K$ is the Jacobian of the transformation $\boldsymbol{F}_K$. A direct computation reveals that

$$D\boldsymbol{F}_K(\hat{\boldsymbol{x}}) = D\boldsymbol{F}_K(\mathbf{0}) + \boldsymbol{\delta}_K \otimes \boldsymbol{w} \tag{57}$$

where $\otimes$ denotes the outer product, $\boldsymbol{w}$ is the vector $(\hat{x}_2, \hat{x}_1)^\top$ and

$$\boldsymbol{\delta}_K = \frac{1}{4}(\boldsymbol{x}_1 - \boldsymbol{x}_2 + \boldsymbol{x}_3 - \boldsymbol{x}_4).$$

where $\boldsymbol{x}_1, \ldots, \boldsymbol{x}_4$ denote the vertices of K enumerated in an anti-clockwise sense. The vector $\boldsymbol{\delta}_K$ may be related to the distance between the midpoints of the lines joining diagonally opposite vertices to one another (see Fig. 2). Obviously, this quantity vanishes in the case of an affine element.

Assumptions (3) and (4) mean that the matrix $\boldsymbol{G}_K$ is invertible everywhere on S, and in particular $\boldsymbol{G}_K(\mathbf{0})$ is invertible. The following result gives quantitative bounds comparing the matrix $\boldsymbol{G}_K$ and its determinant at a general point $\hat{\boldsymbol{x}} \in S$ with the corresponding quantities evaluated at the centroid of S. The bound involves the length $\widehat{\delta}_K$ of the vector $D\boldsymbol{F}_K(\mathbf{0})^{-1}\boldsymbol{\delta}_K \in S$ which may be interpreted as the pre-image of the vector $\boldsymbol{\delta}_K$ on the reference element. As such, $\widehat{\delta}_K$ is independent of any mesh-size and depends purely on the shape of the physical element. The actual numerical value of $\widehat{\delta}_K$ on a particular element is readily evaluated within the standard finite element routines.

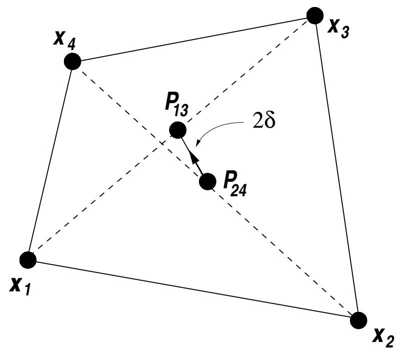

FIGURE 2. Geometric interpretation of the vector $\boldsymbol{\delta}_K$ joining the midpoints P_{13} and P_{24} between opposite vertices of physical element

Lemma 7. *Let*

$$\widehat{\delta}_K = \|D\boldsymbol{F}_K(\mathbf{0})^{-1}\boldsymbol{\delta}_K\|_1. \tag{58}$$

where $\|\cdot\|_1$ *denotes the vector norm on* $\mathbb{R}^2$ *defined by* $\|\boldsymbol{w}\|_1 = |w_1| + |w_2|$. *If* $\widehat{\delta}_K \in [0,1)$, *then for all* $\hat{\boldsymbol{x}} \in S$ *there holds*

$$(1-\widehat{\delta}_K)\det(D\boldsymbol{F}_K(\mathbf{0})) \le \det(D\boldsymbol{F}_K(\hat{\boldsymbol{x}})) \le (1+\widehat{\delta}_K)\det(D\boldsymbol{F}_K(\mathbf{0})) \tag{59}$$

and

$$(1-\widehat{\delta}_K)\boldsymbol{G}_K(\mathbf{0}) \le \boldsymbol{G}_K(\hat{\boldsymbol{x}}) \le (1-\widehat{\delta}_K)^{-1}\boldsymbol{G}_K(\mathbf{0}). \tag{60}$$

Proof. Note that the results are trivially true if $\boldsymbol{\delta}_K$ vanishes and we therefore assume the contrary. Moreover, note that for any vector $\boldsymbol{v} \in \mathbb{R}^2$, we have $\boldsymbol{w}^\top\boldsymbol{v} = \hat{x}_2 v_1 + \hat{x}_1 v_2$ and the extrema of this quantity over $\hat{\boldsymbol{x}} \in S$ are given by $\pm\|\boldsymbol{v}\|_1$, and are attained when $\hat{x}_1 = \pm\operatorname{sgn}(v_2)$ and $\hat{x}_2 = \pm\operatorname{sgn}(v_1)$. The bounds for the determinant are then an easy consequence of the following identity readily obtained from (57)

$$\det(D\boldsymbol{F}_K(\hat{\boldsymbol{x}})) = (1+\kappa(\hat{\boldsymbol{x}}))\det(D\boldsymbol{F}_K(\mathbf{0})) \tag{61}$$

valid for all $\hat{\boldsymbol{x}} \in S$, where

$$\kappa(\hat{\boldsymbol{x}}) = \boldsymbol{w}^\top D\boldsymbol{F}_K(\mathbf{0})^{-1}\boldsymbol{\delta}_K \in [-\widehat{\delta}_K, \widehat{\delta}_K], \quad \hat{\boldsymbol{x}} \in S.$$

Fix $\hat{\boldsymbol{x}} \in S$ and let $\boldsymbol{C}_K$ denote the matrix

$$\boldsymbol{C}_K = (1+\kappa(\hat{\boldsymbol{x}}))^{-1/2} D\boldsymbol{F}_K(\hat{\boldsymbol{x}}) D\boldsymbol{F}_K(\mathbf{0})^{-1},$$

then using identity (57), it is not difficult to see that the eigensolutions of $\boldsymbol{C}_K$ are given by

$$\begin{aligned} \boldsymbol{v}_1 &= D\boldsymbol{F}_K(\mathbf{0})\boldsymbol{w}^\perp, & \lambda_1 &= (1+\kappa(\hat{\boldsymbol{x}}))^{-1/2}; \\ \boldsymbol{v}_2 &= \boldsymbol{\delta}_K, & \lambda_2 &= (1+\kappa(\hat{\boldsymbol{x}}))^{1/2}. \end{aligned}$$

Thus, the spectral radius of the matrix $\boldsymbol{C}_K$ is given by

$$\rho(\boldsymbol{C}_K) = \max_{\hat{\boldsymbol{x}}\in S}\left((1+\kappa(\hat{\boldsymbol{x}}))^{1/2}, (1+\kappa(\hat{\boldsymbol{x}}))^{-1/2}\right) = \left(1-\widehat{\delta}_K\right)^{-1/2}.$$

Now, observe that thanks to (61),

$$\begin{aligned}\boldsymbol{C}_K^\top \boldsymbol{C}_K &= \frac{1}{1+\kappa(\hat{\boldsymbol{x}})}(D\boldsymbol{F}_K(\hat{\boldsymbol{x}})D\boldsymbol{F}_K(\mathbf{0})^{-1})^\top (D\boldsymbol{F}_K(\hat{\boldsymbol{x}})D\boldsymbol{F}_K(\mathbf{0})^{-1}) \\ &= \frac{\det(D\boldsymbol{F}_K(\mathbf{0}))}{\det(D\boldsymbol{F}_K(\hat{\boldsymbol{x}}))}(D\boldsymbol{F}_K(\hat{\boldsymbol{x}})D\boldsymbol{F}_K(\mathbf{0})^{-1})^\top (D\boldsymbol{F}_K(\hat{\boldsymbol{x}})D\boldsymbol{F}_K(\mathbf{0})^{-1}) \\ &= \det(D\boldsymbol{F}_K(\mathbf{0}))\, D\boldsymbol{F}_K(\mathbf{0})^{-\top}\boldsymbol{G}_K(\hat{\boldsymbol{x}})D\boldsymbol{F}_K(\mathbf{0})^{-1}.\end{aligned}$$

Hence, on rearranging and bounding in terms of the spectral radius, we obtain

$$\boldsymbol{G}_K(\hat{\boldsymbol{x}}) \le \rho(\boldsymbol{C}_K)^2 \boldsymbol{G}_K(\mathbf{0})$$

and the upper bound follows on inserting the bound for the spectral radius. The lower bound follows in a similar fashion on observing that

$$\boldsymbol{C}_K^{-1}\boldsymbol{C}_K^{-\top} = \det(D\boldsymbol{F}_K(\mathbf{0}))^{-1} D\boldsymbol{F}_K(\mathbf{0})\boldsymbol{G}_K(\hat{\boldsymbol{x}})^{-1} D\boldsymbol{F}_K(\mathbf{0})^\top$$

and that the spectral radius of $\boldsymbol{C}_K^{-1}$ coincides with that of $\boldsymbol{C}_K$. □

References

[1] M. Ainsworth, Robust a posteriori error estimation for non-conforming finite element approximation, *SIAM J. Numer. Anal.*, accepted for publication.

[2] M. Ainsworth and J.T. Oden, *A Posteriori Error Estimation in Finite Element Analysis*, Pure and Applied Mathematics. Wiley-Interscience, John Wiley & Sons, New York, 2000.

[3] I. Babuska and T. Strouboulis, *The finite element method and its reliability*, Numerical mathematics and scientific computation, Oxford University Press, Oxford, 2001.

[4] I. Babuska and M. Suri, On locking and robustness in the finite element method, *SIAM J. Numer. Anal.*, 29:1261–1293, 1992.

[5] C. Carstensen, S. Bartels and S. Jansche, A posteriori error estimates for nonconforming finite element methods, *Numer. Math.*, 92(2):233–256, 2002.

[6] C. Carstensen and S. A. Funken, Constants in Clément-interpolation error and residual based a posteriori error estimates in finite element methods, *East-West J. Numer. Math.*, 8(3):153–175, 2000.

[7] P. G. Ciarlet, *The Finite Element Method for Elliptic Problems*, Elsevier, North-Holland, 1978.

[8] M. Crouzeix and P. A. Raviart, Conforming and nonconforming finite element methods for solving the stationary Stokes equations, *RAIRO Modél. Math. Anal. Numér.*, 3:33–75, 1973.

[9] E. Dari, R. Duran and C. Padra, Error estimators for nonconforming finite-element approximations of the Stokes problem, *Math. Comp.*, 64(211):1017–1033, July 1995.

[10] E. Dari, R. Duran, C. Padra and V. Vampa, A posteriori error estimators for nonconforming finite element methods, *RAIRO Modél. Math. Anal. Numér.*, 30(4):385–400, 1996.

[11] R. H. W. Hoppe and B. Wohlmuth, Element-oriented and edge-oriented local error estimators for nonconforming finite element methods, *RAIRO Modél. Math. Anal. Numér.*, 30:237–263, 1996.

[12] Pingbing Ming and Zhong-Ci Shi, Quadrilateral mesh, *Chinese Ann. Math. Ser. B*, 23(2):235–252, 2002.

[13] Pingbing Ming and Zhong-Ci Shi, Quadrilateral mesh revisited, *Comput. Methods Appl. Mech. Engrg.*, 191(49-50):5671–5682, 2002.

[14] R. Rannacher and S. Turek, Simple nonconforming quadrilateral Stokes element, *Numer. Meth. PDE.*, 8(2):97–111, 1992.

[15] R. Verfurth. *A review of a posteriori error estimation and adaptive mesh refinement techniques*, Wiley-Teubner, 1996.

Mathematics Department, Strathclyde University, 26 Richmond Street, Glasgow G1 1XH, Scotland.

E-mail: `M.Ainsworth@strath.ac.uk`

URL: `http://www.maths.strath.ac.uk/~aas98107`